Chemical Engineering Journal 145 (2009) 429–435

Contents lists available at ScienceDirect

Chemical Engineering Journal

journal homepage: www.elsevier.com/locate/cej

Development of a microstructured reactor for heterogeneously catalyzed gas phase reactions: Part II. Reactor characterization and kinetic investigations

O. Schwarz [a], P.-Q. Duong [b], G. Schäfer [b], R. Schomäcker [a,*]

[a] Department of Chemistry, Technical University of Berlin, Straße des 17. Juni 124-128, D-10623 Berlin, Germany
[b] Atotech Deutschland GmbH, Erasmusstraße 20, D-10553 Berlin, Germany

ARTICLE INFO

Article history:
Received 1 July 2008
Received in revised form
15 September 2008
Accepted 17 September 2008

Keywords:
Microstructured reactor
Heterogeneous catalysis
Oxidative dehydrogenation
Propane
ODP
Residence time distribution
Kinetics
Oxygen distribution

ABSTRACT

A new type of microstructured reactor was characterized and tested in the oxidative dehydrogenation of propane (ODP) with respect to reaction engineering aspects. Residence time behavior was measured using O_2/N_2 step injection experiments and theoretically analyzed by applying the axial dispersion model, resulting in Bodenstein numbers in the range of 70. Catalytic performance in the ODP was predicted on the basis of a kinetic model from the literature, showing good agreement for low degrees of propane conversion. In order to elucidate discrepancies between experimental and forecasted model data at higher degrees of propane conversion (i.e., >12.5%), possible sources of error were systematically investigated. Specifically, heat and mass transport limitations were excluded as well as possible inaccuracies of the applied kinetic model were examined. It could be shown that microstructured reactors are well suited to be applied for strongly exothermic heterogeneously catalyzed gas phase reactions since they allow isothermal reaction conditions over a wide range of concentrations and temperatures.

© 2008 Elsevier B.V. All rights reserved.

1. Introduction

The potential of microreaction technology (MRT) for substantially improving the efficiency of chemical production processes has long been promoted in the literature. Over the last two decades, many studies have been done on various reactions using innumerous reactor designs specifically developed for a whole range of unit operations [1–8]. However, most research activities were focused on lab-scale applications with only few attempts to enter industrial-scale production regimes. One of the most regarded examples is the DEMiS project, which was designed to prove the principle applicability of microstructured reactors for industrial processes [9]. In order to widen the range of available reactor designs for larger production scales, a scalable manufacturing concept for microstructured reactors was developed prior to this work. The results were presented in detail in Part I of this paper.

The oxidative dehydrogenation of propane (ODP) to propene was chosen as a sensitive test reaction, since it is fast and strongly exothermic and therefore well suited to be applied in a microstructured reactor [10–12]. It has been intensively investigated during the past but the major challenge in the development process being the formulation of a catalyst with sufficient propene selectivity has not been overcome yet [13–18]. However, the simultaneous development of innovative reaction technologies and new catalyst formulations might lead to an economically feasible process for the ODP finally.

In the first step, our microstructured reactors were tested with respect to reaction engineering aspects that might be useful to improve the overall process efficiency of the ODP once a promising catalyst system has been found. Especially, residence time distributions and catalytic behavior were investigated. Experimental results were compared to a kinetic model published by Frank et al. [19] in order to verify the potential of microstructured reactors for fast and strongly exothermic heterogeneously catalyzed gas phase reactions. In particular, the usefulness of a distributed oxygen feed was analyzed.

2. Experimental

All catalytic coatings and microstructured reactors were fabricated according to the detailed descriptions in Part I of this paper. For sake of brevity, specifics on the preparation and characterization of the coatings and the manufacturing process of the reactor modules will not be repeated here.

* Corresponding author. Tel.: +49 30 314 249 73; fax: +49 30 314 215 95.
E-mail address: schomaecker@tu-berlin.de (R. Schomäcker).

1385-8947/$ – see front matter © 2008 Elsevier B.V. All rights reserved.
doi:10.1016/j.cej.2008.09.035

Nomenclature

A_W	heat transfer area (m^2)
Bo	Bodenstein number
c_i	concentration of component i ($mol\,l^{-1}$)
c_p	specific heat capacity ($J\,kg^{-1}\,K^{-1}$)
D_{ax}	axial dispersion coefficient ($m^2\,s^{-1}$)
D_e	effective diffusion coefficient ($m^2\,s^{-1}$)
D_i	molecular diffusion coefficient ($m^2\,s^{-1}$)
$E(\theta)$	residence time distribution function
$E_{A,i}$	activation energy of reaction i ($J\,mol^{-1}$)
$F(\theta)$	cumulative residence time distribution function
$\Delta_R H_i$	reaction enthalpy of reaction i ($J\,mol^{-1}$)
k_W	overall heat transfer coefficient ($J\,s^{-1}\,m^{-2}\,K^{-1}$)
k_∞	pre-exponential factor (with reaction order m) (s^{-1} $(m^3\,mol^{-1})^{m-1}$)
L	reactor length (m)
m_i	reaction order for hydrocarbons of reaction i
n_i	reaction order for oxygen of reaction i
N	number CSTRs in cascade
r_m	reaction rate normalized by catalyst mass ($mol\,kg^{-1}\,s^{-1}$)
$(r_{eff})_S$	effective reaction rate normalized by catalyst surface ($mol\,m^{-2}\,s^{-1}$)
$(r_{eff})_V$	effective reaction rate normalized by reactor volume ($mol\,m^{-3}\,s^{-1}$)
R	universal gas constant (8.314) ($J\,mol^{-1}\,K^{-1}$)
R_0	hydraulic diameter (m)
t	effective residence time (s)
T	reaction temperature (°C, K)
T_W	temperature of reactor wall (°C, K)
u_x	linear flow velocity ($m\,s^{-1}$)
V_R	reactor volume (m^3)

Greek letters

δ_{Cat}	thickness of catalytic coating (μm)
θ	reduced residence time
ρ	specific density ($kg\,m^{-3}$)
$\tau_{Cascade}$	mean residence time of cascade of CSRTs (s)
τ_{hyd}	hydrodynamic residence time (s)
τ_{mod}	modified residence time ($kg\,s\,m^{-3}$)
τ_{MR}	mean residence time of microstructured reactor (s)
τ_{PFTR}	mean residence time of PFTR (s)

2.1. Reactor designs

In addition to the structured steel platelets that were introduced before (single channel design, 35 mm length, 21 mm width, 0.23 mm depth), a multi-channel platelet (54 mm length, 1 mm width, 0.3 mm depth, 0.55 mm wall thickness, 22 channels) was used for manufacturing the microstructured reactors. Furthermore, the multi-channel design was adapted to distribute the oxygen feed over the catalyst bed opposed to the conventional co-feed mode of reactants (i.e., the platelet was perforated with 22 equally spaced holes in each channel with an average diameter of 0.5 mm). With this reactor configuration, C_3H_8 and N_2 are fed to the catalyst-coated channels whereas O_2 is fed separately through the perforated channels. Fig. 1a shows a schematic drawing of the multi-channel microstructured reactor, whereas Fig. 1b shows a photograph of a reactor between two brass metal plates equipped with four heating cartridges.

Thermal behavior of the microstructured reactors (only in case of the single channel design) was monitored using three thermocouples that were placed in equal distances along the catalyst bed. Temperature was controlled by a fourth thermocouple that was placed in some distance from the catalyst-coated channels (for more details see Part I of this paper). In case of the multi-channel design, a thermocouple for temperature control was placed in one of the heating plates.

2.2. Flow characteristics

Residence time behavior of the different reactor designs was recorded at room temperature using O_2/N_2 step injection experiments (flow rate 60 $ml_n\,min^{-1}$). For changing the flow from oxygen to nitrogen, a four-way cross-flow valve was used. Signals were detected by a mass spectrometer (InProcess Instruments GAM200). The reactors were directly attached to the cross-flow valve and the mass spectrometer via two connectors (1/8 in. at valve outlet and mass spectrometer inlet to 6 mm at reactor in- and outlet, respectively). For blind tests, the reactors were removed and the connectors were directly linked with each other. Thereby, the influence of the mass spectrometer and the tubing on the recorded residence time distribution can be separated from the influence of the microstructured reactors. For quantitative analysis of the residence time experiments, the axial dispersion model was combined with a PFTR and a cascade of CSTRs in order to fit experimental data and extract corresponding Bodenstein numbers for all examined reactor designs. The residence time distribution (RTD) function $E(\theta)$ and the cumulative RTD function $F(\theta)$ of the axial dispersion model are given according to the following equations [20]:

$$E(\theta) = \frac{1}{2}\sqrt{\frac{\mathrm{Bo}}{\pi\theta}}\,\exp\left(-\frac{(1-\theta)^2\,\mathrm{Bo}}{4\theta}\right) \tag{1}$$

$$F(\theta) = \frac{1}{2}\left[1 - \mathrm{erf}\left((1-\theta)\sqrt{\frac{\mathrm{Bo}}{4\theta}}\right)\right] \tag{2}$$

where $\theta = t/\tau_{MR}$ is the reduced residence time and $\mathrm{Bo} = (u_x L)/D_{ax}$ is the dimensionless Bodenstein number. Furthermore, t is the effective residence time, τ_{MR} is the mean residence time of the microstructured reactor, D_{ax} is the axial dispersion coefficient, u_x is the linear flow velocity, and L the reactor length. The RTD function $E(\theta)$ and the cumulative RTD function $F(\theta)$ of a cascade of CSTRs are given in the following equations [20]:

$$E(\theta) = \frac{N(N\theta)^{N-1}}{(N-1)!}\,\exp(-N\theta) \tag{3}$$

$$F(\theta) = 1 - \exp\,(-N\theta)\left[\sum_{i=0}^{N-1}\frac{(N\theta)^i}{i!}\right] \tag{4}$$

where $\theta = t/\tau_{Cascade}$ is the reduced residence time, N the number of CSTRs, and $\tau_{Cascade}$ is the mean residence time of the reactor cascade. The software package Berkeley Madonna (Version 8.0.1) was used to numerically fit model curves to experimental data.

2.3. Catalytic behavior

Catalytic measurements were performed using the experimental set up that was described in detail in Part I of this paper. The microstructured reactors were kept between 400 and 500 °C. The ratio of the $C_3H_8/O_2/N_2$ inlet flow was 2/1/4. Total volume flows were varied from 30 to 240 $ml_n\,min^{-1}$. Since organic binder formulations showed least influence on the catalytic behavior of the coatings compared to the reference catalyst, results from inorganic binder formulations were excluded from this part of the present

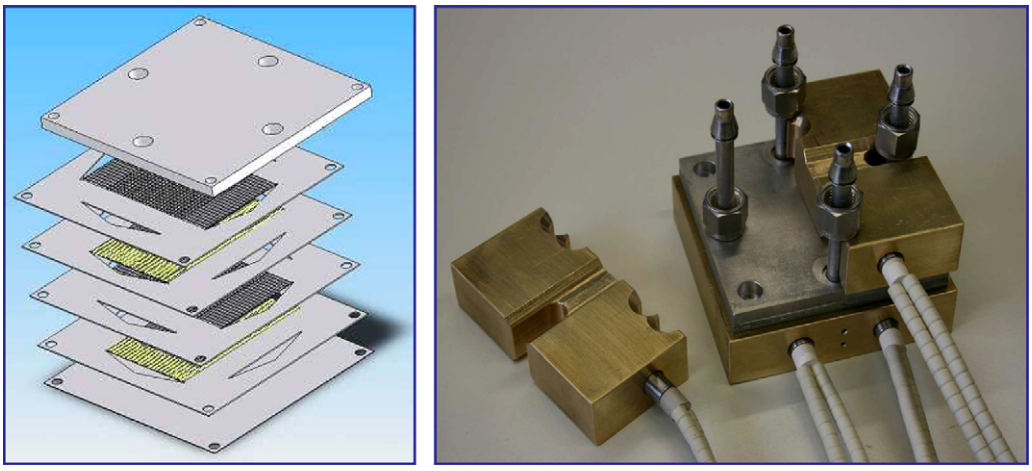

Fig. 1. (a) Schematic drawing of a microstructured reactor for distributing oxygen over the catalyst bed and (b) photograph of a microstructured reactor with heating blocks equipped with heating cartridges.

study. The thickness of the catalytic coatings varied between 5 and 25 μm. All catalytic measurements except for the oxygen distribution reactor were performed using microstructured reactors made from four structured single channel platelets and two platelets for inserting the thermocouples. In case of the oxygen distribution reactor, four multi-channel platelets and four perforated multi-channel platelets were combined without including platelets for temperature control.

3. Results and discussion

3.1. Residence time distributions

The knowledge about residence time behavior of a reactor is crucial for any further reactor modeling. Parameter estimation from experimental data for standardized models, such as the axial dispersion model or the reactor cascade model, is necessary to mathematically describe the behavior of non-ideal reactors. However, deriving model parameters from experimental data for microstructured devices turned out to be problematical, since adequate detectors and theoretical models are still under development [21–26]. Therefore, we do not aim for a highly accurate mathematical description of our reactors but for a sufficiently precise parameter estimate in order to evaluate residence time behavior and select a suitable reactor model. Fig. 2 shows the cumulative RTD functions for all analyzed microstructured reactors (reactors with distributed O_2 feed were excluded from this series of experiments, due to their complex internal geometry, making them difficult to describe with standardized models).

Fitting the axial dispersion model to unadjusted experimental data in order to determine model parameters will result in highly inaccurate parameter estimates, since the mass spectrometer that was used for detecting the cumulative RTD functions also contributed to overall backmixing and residence time (as seen in Fig. 2). Therefore, we combined the axial dispersion model for fitting the reactor behavior with an ideal PFTR to account for the influence of the mass spectrometer and the tubing as follows:

step injection → microstructured reactor → PFTR → detector

Model parameters (τ_{MR}, Bo, and τ_{PFTR}) were simultaneously varied by the software package Berkeley Madonna to fit the combined model to our experimental data. The residence time of the imaginary PFTR τ_{PFTR} was determined to be 9.9 s. Corresponding residence times $\tau_{MR,1}$ of the microstructured reactors varied between 4.6 and 5.2 s. Under these assumptions, all backmixing is assigned to the reactors, resulting in relatively low Bodenstein numbers Bo_1 of 15–19 and relatively high residence times compared to hydrodynamic residence times (τ_{hyd} = reactor volume/flow rate). However, step injection experiments without microstructured reactors showed that a significant proportion of the backmixing is due to the valve system of the mass spectrometer (see Fig. 2). Therefore, our model was modified in order to account for the influence of the mass spectrometer by adding a cascade of CSTRs:

step injection → microstructured reactor → PFTR

→ cascade of CSTRs → detector

In the first step, parameters of the PFTR and the reactor cascade were determined fitting experimental data from blind tests (without microstructured reactors). The influence of the mass spectrometer can be well described by a parameter combination of τ_{PFTR} = 9.5 s, $\tau_{Cascade}$ = 2.9 s and N = 3. These parameters were kept constant for consecutive fits in order to guarantee identical boundary conditions. In the second step, $\tau_{MR,2}$ and Bo_2 were simultaneously varied to fit the combined model to the experimental data. The result of this method is shown in

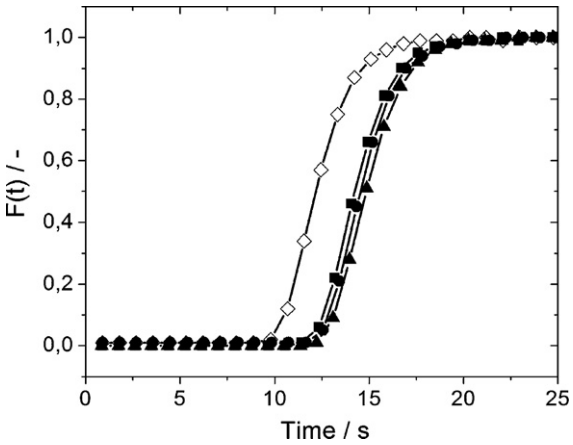

Fig. 2. Response functions of mass spectrometer (◊), single channel designs (■, face-to-back; ●, face-to-face) and multi-channel design (▲) to O_2/N_2 step injection experiments (flow rate 60 ml_n min^{-1}).

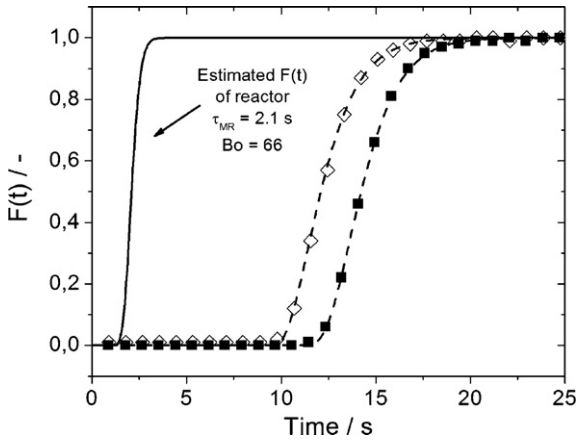

Fig. 3. Fit of adjusted model (dashed lines) to experimental data (■, response function of microstructured reactor including mass spectrometer; ◊, response function of mass spectrometer individually) in order to estimate $\tau_{MR,2}$ and Bo_2 for microstructured reactor (solid line, flow rate 60 $ml_n\ min^{-1}$).

Fig. 3, revealing a good agreement of experimental and model data.

By accounting for the influence of the mass spectrometer on the cumulative RTD function, significantly higher Bodenstein numbers Bo_2 were obtained for the microstructured reactors. Through this method, backmixing effects are proportionally assigned to the mass spectrometer and the microstructured reactors, respectively. Values of Bo_2 vary between 66 and 76, giving justified rise to the assumption that the residence time behavior of our microstructured reactors can be approximated with an ideal PFTR model [20]. In addition, experimental $\tau_{MR,2}$ values fall in the range of hydrodynamic residence times, which is in good accordance with assuming a PFTR model for the microstructured reactors. Results of our residence time experiments are summarized in Table 1.

However, it has to be stressed that this method is not suitable for determining model parameters with high accuracy. This is mainly due to the substantial influence of the detector system on resulting cumulative RTD functions. Sensitivity of parameter estimation is high, making this method prone to misinterpretation. However, it serves the purpose to assess residence time behavior of microstructured devices and to choose a suitable reactor model.

3.2. Kinetic investigations

In order to analyze the catalytic behavior of the tested microstructured reactors, a kinetic model was chosen from the literature to evaluate the potential performance of our reactors in the oxidative dehydrogenation of propane. Frank et al. suggested a simplified power law approach for a low loaded $VO_x/\gamma\text{-}Al_2O_3$ catalyst to mathematically describe their experimental data and extract intrinsic kinetic parameters [19]:

$$r_1 = \frac{dc_{C_3H_8}}{d\tau_{mod}} = k_{\infty,1} \exp\left(-\frac{E_{A,1}}{RT}\right) c_{C_3H_8}^{m_1} c_{O_2}^{n_1} \quad (5)$$

$$r_2 = \frac{dc_{C_3H_6}}{d\tau_{mod}} = k_{\infty,2} \exp\left(-\frac{E_{A,2}}{RT}\right) c_{C_3H_6}^{m_2} c_{O_2}^{n_2} \quad (6)$$

$$r_3 = \frac{dc_{O_2}}{d\tau_{mod}} = -0.5r_1 - 3.5r_2 \quad (7)$$

where r_1 and r_2 are the reaction rates for selective propane conversion and propene deep oxidation, r_3 is the reaction rate for oxygen conversion, and τ_{mod} is the modified residence time (catalyst mass divided by volume flow of reactants). All model parameters were taken as published (i.e., activation energies and reaction orders), except $k_{\infty,1}$ and $k_{\infty,2}$, which were matched to experimental data as reported in [27] in order to adjust for specific catalyst characteristics, such as the surface density of VO_x species. In addition, the accuracy of activation energies was crosschecked with kinetic data from the literature and showed good agreement [28]. All parameters used in the kinetic model are summarized in Table 2.

In order to predict catalytic behavior of our microstructured reactors from intrinsic kinetics, an isothermal PFTR reactor model was chosen. The assumptions inherent to this model are as follows: (1) neither axial nor radial temperature gradients exist along the catalytic bed and (2) no axial backmixing but perfect radial mixing prevails in the reactor. Since residence time behavior experiments revealed Bodenstein numbers in the range of 70, the PFTR reactor type appears to be well suited to mathematically describe the progress of the reaction in our microstructured reactors. In terms of isothermal reaction conditions, no temperature gradients were observed along the catalyst bed measured by three thermocouples that were placed close the coated reactor channels, justifying the above assumptions of an isothermal reactor model.

In the first step, the mass balances given in Eqs. (5)–(7) were solved separately from the heat balance to verify if the experimental data obtained from the microstructured reactors can be described by the assumed kinetics and the applied reactor model. Fig. 4a shows measured and simulated propane conversion versus modified residence time, whereas Fig. 4b shows measured and simulated propene selectivity versus propane conversion.

It can be seen that activity behavior of the microstructured reactors can be simulated with good accuracy for propane conversion degrees <12.5% at 400 and 450 °C. At 500 °C propane conversion could not be kept below 12.5% due to the high activity of the applied catalyst. However, the trend predicts that activity behavior at 500 °C will be described by the model for propane conversion degrees <12.5%, too. Therefore, it can be concluded that the assumed kinetic model is suitable for describing our experimental data from the microstructured reactors. However, once propane conversion is further increased (>12.5%), activity is dramatically overestimated by the model. Similarly, selectivity towards propene can be predicted with good accuracy for low propane conversion degrees but once propane conversion is increased beyond 10%, selectivity is greatly overestimated by the model.

The discrepancy between experimental and predicted model data might be due to several reasons. First of all it has to be verified that isothermal reaction conditions can be assumed for all measurements. As was noted before, no temperature gradients could be observed along the catalyst bed during our experimental studies. In addition, thermal behavior of the microstructured reactors was theoretically modeled by simultaneously solving the mass balances according to Eqs. (5)–(7) and the heat balance according to

Table 1
Residence times (τ_{hyd}, τ_{MR}) and Bodenstein numbers (Bo) of reactor designs determined from parameter estimation. Index 1 corresponds to adapted model with PFTR, index 2 to adapted model with PFTR/CSTRs.

Reactor design	Face-to-back single channel	Face-to-face single channel	Face-to-back multi-channel
τ_{hyd} (s)	1.8	2.1	2.8
$\tau_{MR,1}$ (s)	4.6	4.9	5.2
Bo_1	15	17	19
$\tau_{MR,2}$ (s)	2.1	2.5	2.7
Bo_2	66	73	76

Table 2
Kinetic parameters applied for modeling isothermal microstructured reactor.

	k_∞	E_A (kJ mol^{-1})	m	n
Propane conversion (r_1)	5.816×10^5 mol$^{0.25}$ m$^{2.25}$ kg^{-1} s^{-1}	111	0.65	0.10
Propene combustion (r_2)	5.672×10^5 mol$^{-0.7}$ m$^{5.1}$ kg^{-1} s^{-1}	102	0.70	1.00

Eq. (8):

$$\frac{dT}{d\tau_{mod}} = \frac{-r_1\Delta_R H_1 - r_2\Delta_R H_2}{c_0 c_p} - (T - T_W)\frac{k_W A_W}{V_R c_0 c_p \rho} \quad (8)$$

where $\Delta_R H_1 = -117.6$ kJ mol^{-1} and $\Delta_R H_2 = -1360.2$ kJ mol^{-1} are the reaction enthalpies of Reactions (1) and (2), c_0 is the initial total gas concentration, and c_p and ρ are the average heat capacity and density of the gases estimated from the literature [29]. Furthermore, T_W is the temperature of the reactor wall, k_W is the estimated heat transfer coefficient, A_W the heat transfer area and V_R the reactor volume. Fig. 5 shows the temperature gradient, propane and oxygen conversion along the catalyst bed in a microstructured reactor (single channel design) at 500 °C.

Applying conservative estimates for k_W (50 W m^{-2} K^{-1}) and A_W (1.47×10^{-3} m^2), the maximum temperature rise along the catalyst bed is less than 1 K at full oxygen conversion. Therefore, it can be concluded that isothermal reaction conditions prevail in all experimental series.

Another possible reason for overestimating the activity of the microstructured reactors might be the existence of mass transport limitations, decreasing experimentally determined propane conversion. In order to estimate the influence of possible mass transport limitations, two diagnostic criteria were applied. For evaluating external and internal mass transport limitations, the Mears criterion [20,30] according to Eq. (9) and the Weisz–Prater criterion [20,31] according to Eq. (10) adjusted for planar catalyst layers were used:

$$\frac{R_0(r_{eff})_S}{D_i c_0} < 0.05 \quad (9)$$

$$\frac{\delta_{Cat}^2(r_{eff})_V}{D_e c_0} < 0.07 \quad (10)$$

where R_0 is the hydraulic diameter of the channel, D_i is the molecular diffusion coefficient, D_e is the effective diffusion coefficient, δ_{Cat} is the thickness of the catalytic coating, $(r_{eff})_S$ is the reaction rate normalized by the catalyst surface, and $(r_{eff})_V$ is the reaction rate normalized by the reactor volume. The Mears and Weisz-Prater criteria were evaluated for reaction rate r_1 at 500 °C using parameters provided in Table 2 and a coating thickness of 25 μm. The left hand side of Eqs. (9) and (10) were calculated to be 9.8×10^{-6} and 8.7×10^{-4}, respectively. Both values are far below the given limits for an irreversible first-order reaction. Therefore, it is unlikely that mass transport phenomena limit propane conversion in the microstructured reactors and are responsible for the discrepancies between experimental and simulated data.

Since the kinetic model by Frank et al. was developed exclusively from differential measurements of propane and propene conversion, it might well be possible that some of their model parameters are not representative for higher degrees of propane conversion. Especially, the overestimated activity might be due to a wrong reaction order for oxygen in Reaction (1). It was estimated to be 0.1, which limits the influence of oxygen concentration on the reaction rate. However, it is obvious that the consumption of propane strongly decreases with decreasing oxygen concentrations, which gives rise to the assumption that n_1 was underestimated in the applied kinetic model.

In addition to the discrepancies between experimental and simulated data for activity behavior of the microstructured reactors,

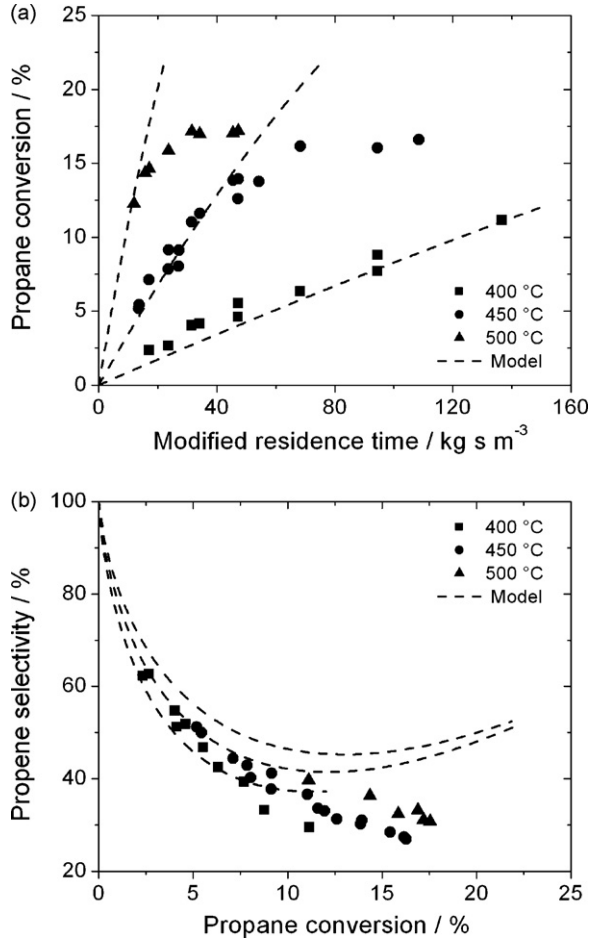

Fig. 4. Comparison of predicted model data with experimental data for (a) propane conversion and (b) propene selectivity ($C_3H_8/O_2/N_2 = 2/1/4$, flow rate 30–240 ml$_n$ min^{-1}).

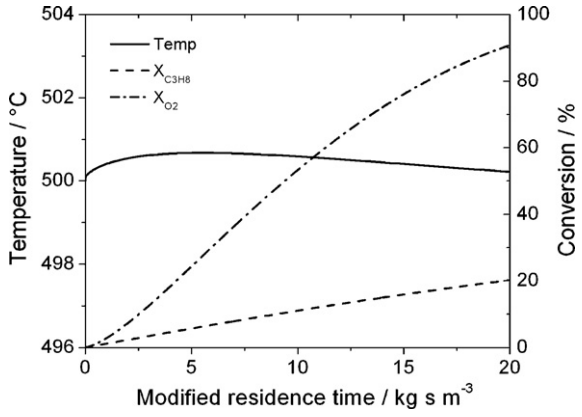

Fig. 5. Simulated temperature gradient and conversion degrees of propane and oxygen along the catalytic bed in a microstructured reactor ($C_3H_8/O_2/N_2 = 2/1/4$, flow rate 30–240 ml$_n$ min^{-1}).

also selectivity towards propene cannot be forecasted with satisfactory accuracy. As was shown in Fig. 4b, selectivity is predicted to decrease to a minimum and subsequently increase at high degrees of propane conversion. This catalytic behavior was not observed during any experimental series while using our microstructured reactors. The prediction of the rising propene selectivity is based on the difference between reaction orders for oxygen in Reaction (1) and (2). Reaction order n_1 was estimated to be 0.1, whereas reaction order n_2 was estimated to be 1.0. This difference in reaction orders leads to a relatively high reaction rate r_1 in comparison to reaction rate r_2 at low oxygen concentrations. Therefore, selectivity towards propene is forecasted to increase at high degrees of propane conversion. In order to verify or falsify the assumption that n_1 and n_2 are different from each other, the microstructured reactor with the distributed oxygen feed was applied. If n_1 is smaller than n_2, lowering the oxygen partial pressure at the catalytically active sites should increase propene selectivity. This behavior was also theoretically examined in the literature [32]. Fig. 6 shows experimental data from a conventional co-feed reactor and the oxygen distribution reactor as well as corresponding simulated selectivity-conversion trajectories.

It can be seen that experimental data from both reactor types are almost identical in terms of selectivity behavior. In contrast, propene selectivity predicted from the simulation of the oxygen distribution reactor is far higher than for the conventional co-feed reactor. Therefore, there are strong experimental and theoretical indications that oxygen reaction orders n_1 and n_2 are not as different as proposed by Frank et al. There are several reasons why their model is not able to predict concentrations for high degrees of propane conversion. In their experiments, propane and propene conversion degrees were kept to values <2% and <3%, respectively. The main reason for that was the inability to control temperature gradients along the catalyst bed. In addition, simplifications such as the assumption of a constant CO:CO_2 ratio might not be justified. Most importantly, activation energies of both reactions were not determined in the same temperature range, whereas reaction orders were assumed to be independent from temperature. However, the model serves well for the purpose it was developed for but seems unsuitable for extrapolation. As was explained above, it appears most likely that oxygen reaction orders are rather similar. Therefore, another simulation was performed for values of $n_1 = n_2$ of 1.0 and 0, respectively, in order to evaluate if a better agreement with the experimental data can be achieved (in both cases, pre-exponential factors had to be slightly adjusted in order to correct for the change in reaction orders). Fig. 7a shows experimental and simulated propane conversion versus modified residence time at 450 °C for reaction orders $n_1 = n_2 = 1.0$ and 0 ($k_{\infty,1} = 2.99 \times 10^5$, $k_{\infty,2} = 4.68 \times 10^5$ for $n = 1.0$ and $k_{\infty,1} = 2.93 \times 10^5$, $k_{\infty,2} = 4.17 \times 10^5$ for $n = 0$). In comparison, Fig. 7b shows experimental and simulated selectivity-conversion trajectories at 450 °C, also for reaction orders $n_1 = n_2 = 1.0$ and 0.

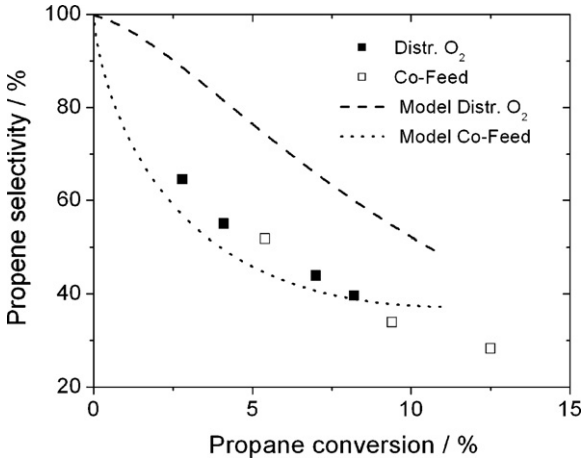

Fig. 6. Comparison of predicted model data with experimental data for co-feed mode of reactants and distributed oxygen feed (450 °C, $C_3H_8/O_2/N_2 = 2/1/4$, total flow rate 30–240 $ml_n\ min^{-1}$).

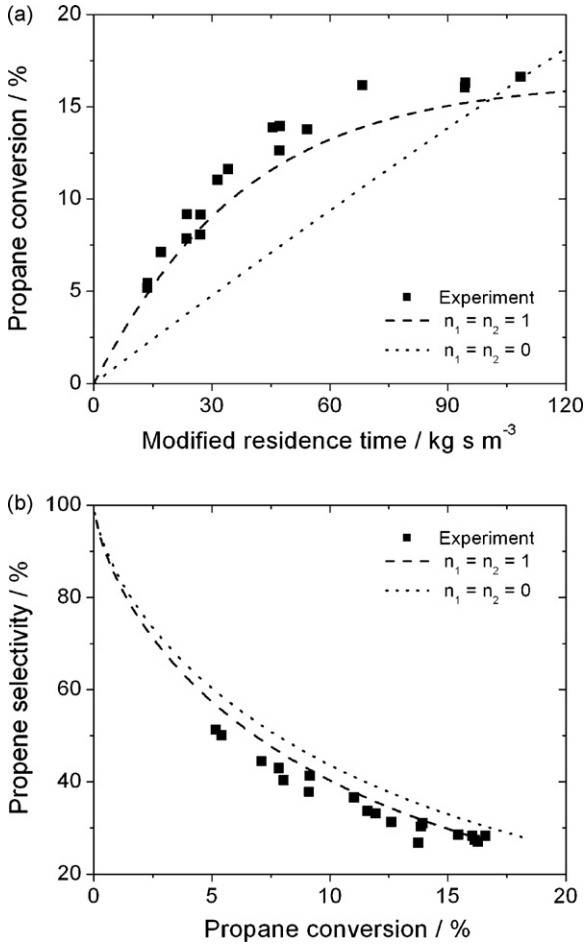

Fig. 7. Theoretical propane conversion (a) and propene selectivity (b) for adjusted oxygen reaction orders compared to experimental data (450 °C, $C_3H_8/O_2/N_2 = 2/1/4$, flow rate 30–240 $ml_n\ min^{-1}$).

If both reaction orders are set to 1.0, activity behavior can be described more precisely than with the original model. The loss of activity at higher degrees of propane conversion is accounted for, since reaction rate r_1 experiences a higher dependency on oxygen concentration compared to the original model by Frank et al., where n_1 was determined to be 0.1. If both reaction orders are set to 0, the agreement between experimental and simulated data becomes worse, which is due to the same reason as above. The loss of activity due to unavailability of oxygen is not taken into account, since in this case reaction rates are independent of the oxygen concentration. In case of selectivity behavior, both cases yield a more accurate prediction of experimental data. Selectivity-conversion trajectories monotonically decrease, without showing increasing propene selectivity at high degrees of propane conversion. However, it has to be noted that these insights have to be experimentally verified. So far, there are only strong indications that oxygen reaction orders have to be very similar. This result is also supported by the literature [33].

4. Summary

Our microstructured reactors were characterized in the oxidative dehydrogenation of propane with respect to reaction engineering aspects. It was shown that this type of reactor experiences only minor backmixing, since Bodenstein numbers are in the range of 70. Furthermore, it could be experimentally and theoretically verified that isothermal reaction conditions can be achieved over a wide temperature range, making microstructured reactors excellent tools for controlling strongly exothermic reactions. In comparison to conventional reactor technologies, they are advantageous with respect to their superior heat transfer properties.

In order to assess the prospective catalytic performance of our microstructured reactors, a kinetic model from the literature was applied to predict propane conversion and propene selectivity. It was shown that the full kinetic potential can be exploited due to the well controllable reactor behavior. However, it was also found that the applied kinetic model is not suitable for extrapolation mainly due to the inability to correctly predict activity and selectivity for high propane conversion degrees. Furthermore, it was shown that a distributed oxygen feed in the oxidative dehydrogenation of propane is not beneficial since oxygen reaction orders appear to be very similar for both consecutive reactions.

With this study, the basis for a detailed kinetic investigation of the chosen model reaction was established, since microstructured reactors are well suited to analyze strongly exothermic heterogeneously catalyzed gas phase reactions under isothermal reaction conditions in a wide range of concentrations and temperatures. Typical problems with challenging reactions such as inefficient heat transfer can be avoided, resulting in more accurate kinetic parameters.

Acknowledgements

Financial support by the “Deutsche Forschungsgemeinschaft (DFG)” as part of the collaborative research centre “Structure, dynamics and reactivity of transition metal oxide aggregates” (Sonderforschungsbereich 546) and by the “Fonds der Chemischen Industrie (FCI)” is acknowledged. In addition, O. Schwarz would like to thank the State of Berlin for providing a NaFöG scholarship. Furthermore, fruitful discussions with Prof. P. Hugo and T. Otremba greatly improved the analysis of our kinetic investigations.

References

[1] W. Ehrfeld, V. Hessel, H. Löwe, Microreactors, Wiley-VCH, Weinheim, 2000.
[2] W. Ehrfeld, V. Hessel, V. Haverkamp, Ullmann’s Encyclopedia of Industrial Chemistry, Electronic Release, Wiley-VCH, Weinheim, 2002.
[3] A. Gavriilidis, P. Angeli, E. Cao, K.K. Yeong, Y.S.S. Wan, Chem. Eng. Res. Des. 80 (2002) 3–30.
[4] V. Hessel, H. Löwe, Chem. Eng. Technol. 26 (2003) 13–24.
[5] V. Hessel, H. Löwe, Chem. Eng. Technol. 26 (2003) 391–408.
[6] V. Hessel, H. Löwe, Chem. Eng. Technol. 26 (2003) 531–544.
[7] E. Klemm, M. Rudek, G. Markowz, R. Schütte, in: R. Dittmeyer, W. Keim, G. Kreysa, A. Oberholz (Eds.), Winnacker/Küchler—Chemische Technik, Band 2: Neue Technologien, 5th ed., Wiley-VCH, Weinheim, 2004, pp. 759–819.
[8] K. Jähnisch, V. Hessel, H. Löwe, M. Baerns, Angew. Chem. 116 (2004) 410–451.
[9] G. Markowz, S. Schirrmeister, J. Albrecht, F. Becker, R. Schütte, K.J. Caspary, E. Klemm, Chem. Eng. Technol. 76 (2004) 620–625.
[10] G. Veser, G. Friedrich, M. Freygang, R. Zengerle, Stud. Surf. Sci. Catal. 122 (1999) 237–245.
[11] N. Steinfeldt, N. Dropka, D. Wolf, M. Baerns, Chem. Eng. Res. Des. 81 (2003) 735–743.
[12] E. Klemm, H. Döring, A. Geißelmann, S. Schirrmeister, Chem. Ing. Tech. 79 (2007) 697–706.
[13] E.A. Mamedov, V.C. Corberán, Appl. Catal. A: Gen. 127 (1995) 1–40.
[14] I.E. Wachs, B.M. Weckhuysen, Appl. Catal. A: Gen. 157 (1997) 67–90.
[15] T. Blasco, J.M. López Nieto, Appl. Catal. A: Gen. 157 (1997) 117–142.
[16] M. Baerns, O. Buyevskaya, Catal. Today 45 (1998) 13–22.
[17] B.M. Weckhuysen, D.E. Keller, Catal. Today 78 (2003) 25–46.
[18] F. Cavani, N. Ballarini, A. Cericola, Catal. Today 127 (2007) 113–131.
[19] B. Frank, A. Dinse, O. Ovsitser, E.V. Kondratenko, R. Schomäcker, Appl. Catal. A: Gen. 323 (2007) 66–76.
[20] G. Emig, E. Klemm, Technische Chemie—Einführung in die Chemische Reaktionstechnik, 5th ed., Springer-Verlag, Berlin, 2005, pp. 444–467.
[21] J.-M. Commenge, L. Falk, J.-P. Corriou, M. S Matlosz, in: M. Matlosz, W. Ehrfeld, J.P. Baselt (Eds.), Microreaction Technology: Proceedings of the Fifth International Conference on Microreaction Technology IMRET 5, Springer-Verlag, Berlin, 2002, pp. 131–140.
[22] P. Pfeifer, L. Bohn, O. Görke, K. Haas-Santo, U. Schygulla, K. Schubert, Chem. Ing. Tech. 76 (2004) 607–613.
[23] F. Trachsel, A. Günther, S. Khan, K.F. Jensen, Chem. Eng. Sci. 60 (2005) 5729–5737.
[24] M. Hoffmann, M. Schlüter, N. Räbiger, Chem. Ing. Tech. 79 (2007) 1067–1075.
[25] S. Lohse, M. Arnold, J. Franzke, D.W. Agar, Chem. Ing. Tech. 79 (2007) 1296.
[26] T. Stief, U. Schygulla, H. Geider, O.-U. Langer, E. Anurjew, J. Brandner, Chem. Eng. J. 135 (2008) 191–198.
[27] O. Schwarz, B. Frank, C. Hess, R. Schomäcker, Catal. Commun. 9 (2008) 229–233.
[28] M.D. Argyle, K. Chen, A.T. Bell, E. Iglesia, J. Catal. 208 (2002) 139–149.
[29] R.C. Weast, G.L. Tuve (Eds.), Handbook of Chemistry and Physics, 48th ed., The Chemical Rubber Co., Cleveland (Ohio), 1967.
[30] D.E. Mears, Ind. Eng. Chem. Proc. Des. Dev. 10 (1971) 541–547.
[31] P.B. Weisz, Z. Phys. Chem. 11 (1957) 1.
[32] C. Hamel, S. Thomas, K. Schädlich, A. Seidel-Morgenstern, Chem. Eng. Sci. 58 (2003) 4483–4492.
[33] A. Bottino, G. Capannelli, A. Comite, S. Storace, R. Di Felice, Chem. Eng. J. 94 (2003) 11–18.